Journal of Applied Polymer Science

Competitive Adsorption of Acid Dyes from Aqueous Solution on Diethylenetriamine-Modified Chitosan Beads

Yikai Yan, Bo Xiang, Xiaowei Yi, Yijiu Li, Qian Jia
Department of Chemistry, Tongji University, Shanghai 200092, China
Correspondence to: B. Xiang (E-mail: bxiangbo@tongji.edu.cn)

ABSTRACT: The interaction between two dyes (AO7 and AG25) during adsorption was studied in detail with diethylenetriamine-modified chitosan beads (CTSN-beads) as the adsorbent. Results indicate that the adsorption capacities and rates were directly related to the molecular size of the dye. The adsorption capacity and rate of AO7 could be greatly weakened by interaction with AG 25 during adsorption, which has a larger molecular size. The adsorption followed the pseudo-second-order kinetic equation and Freundlich model gave a satisfying correlation with the equilibrium data both in the single and binary component system. Adsorption could be divided into three stages, each controlled by different mechanisms. Temperature experiments showed high temperature was beneficial to the mass transfer of dyes. © 2014 Wiley Periodicals, Inc. J. Appl. Polym. Sci. **2014**, *131*, 41168.

KEYWORDS: adsorption; biopolymers and renewable polymers; dyes/pigments; interfaces; surfaces

Received 10 March 2014; accepted 15 June 2014
DOI: 10.1002/app.41168

INTRODUCTION

Many industrial activities, such as textile, leather, paper, rubber, and plastic manufacturing discharge large volumes of wastewater containing various synthetic dyestuffs each year. Even very small amounts of dye in water can be highly visible and undesirable.[1] Most of these dye wastes are also considered toxic and carcinogenic.[2] Additionally, it is rather difficult to biodegrade these dyes in effluent streams due to their aromatic structure, which cause increased accumulation in the environment and can pose a risk to human health. Treatment of dyed effluents has received increasing attention in recent years. Various separation techniques, including adsorption,[3–5] chemical oxidation,[6] membrane filtration,[7] electrochemical techniques,[8] and coagulation[9] have been developed for the removal of dye molecules. Among these physical and chemical methods, adsorption is considered to be the most promising technique because it is simple, quick, and effective.[10]

Chitosan is an abundant, cheap, and biodegradable natural polysaccharide material[11–13] that has been widely employed as an adsorbent for dye removal. However, raw chitosan exhibited limited adsorption capacity because of low specific area.[14,15] Some researchers have also investigated amino groups in chitosan, which are predominant adsorption sites for dyes.[16] It is an effective way to enhance the adsorption of chitosan by introducing more amino groups. In our previous work, porous chitosan beads were synthesized by grafting diethylenetriamine on the surface of chitosan; the results showed that modified chitosan has excellent adsorption efficiency in terms of acid dye molecules.[17]

Up until now, some researchers have studied dye adsorption processes in single component systems. However, limited information has been reported about multicomponent dye adsorption. The study of multi-component dye adsorption presents a major challenge compared with single system due to the complexity of textile effluent and the variability in dyeing processes.[18] Recently, activated carbon and other materials (peat, cypress cone chips, zeolite, and chitosan) have been utilized for the adsorption of dyes from a binary component system.[19–24] Goncalves[25] also used chitosan derivations for the adsorption of Acid Blue 9 and Food Yellow 3 from the binary system with maximum adsorption capacities of 163.6 and 193.4 mg/g, respectively. Noroozi[26] reviewed some applicable models for multicomponent adsorption of dyes. However, to our knowledge, very little information is available about the interaction between dyes during the adsorption process. Thus, in an effort to further investigate the interaction between dyes in binary systems, in this work, diethylenetriamine-modified chitosan beads were synthesized and employed for the adsorption of AO7 and AG25 from a binary component system. Adsorption equilibrium and kinetic models were used for the evaluation of adsorption properties. The effects of time, initial dye concentration, pH and temperature on the interaction between dyes were investigated in a more detailed way to provide the necessary information for its potential application in water treatment.

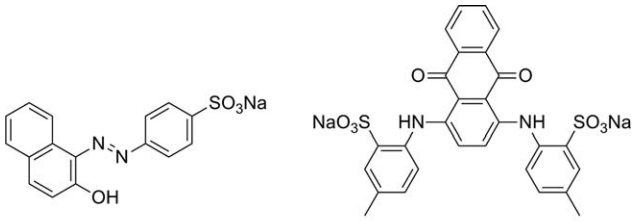

(a) (b)

Figure 1. The structures of (a) Acid Orange 7 and (b) Acid Green 25.

EXPERIMENTAL

Materials

Chitosan (91.2% of deacetylation degree) was provided by the Sinopharm Chemical Reagent Company. AO7 ($M_w = 350.3$ g mol^{-1}; $\lambda_{max} = 485$ nm), AG25 ($M_w = 622.6$ g mol^{-1}; $\lambda_{max} = 642$ nm), and other reagents were all purchased from the Sigma chemical company. All of these chemicals were analytical grade and used without any further purification. All aqueous solutions and standards were prepared using distilled water. The molecule structures of AO7 and AG25 are shown in Figure 1.

Preparation

The CTSN-beads is prepared according to our previous research.[17] First, a chitosan solution was prepared by dissolving 4 g chitosan flakes into 96 g of a 4% (m/m) acetic acid solution. The solution was then dropped from a burette into 800 mL of a sodium hydroxide solution (2 mol L^{-1}) and CTS-beads formed in the shape of uniform balls. Benzaldehyde was slowly added into the mixture of CTS-beads and distilled water for the purpose of protecting amino groups in chitosan. Then, epichlorohydrin and diethylenetriamine were further reacted with the mixture in sequence. The mixture was then dipped into the 2% hydrochloride solution for 48 h to remove the benzaldehyde. Finally, the formed products (CTSN-beads) were washed with distilled water until a neutral pH was reached. The diameters of CTSN-beads are 2.4–2.7 mm.

Adsorption Experiments

Adsorbents (0.016 dry basis of CTSN-beads) with a pH of 4.0 were added to flasks with 50 mL of the dye solution. The dye solution was prepared by dissolving dye in deionized water to the required concentration. The initial concentrations of each dye in single and binary component system are listed in Table I. The flasks were agitated in a water bath (25°C) for 24 h with a shaking speed of 200 rpm. After filtration, the residual concentrations of each dye were measured. Equation (1) was used to calculate the sorption capacity of the absorbent:

Table I. Initial Concentrations of Single and Binary System

	Single system				Binary system	
Dye	1	2	3	4	5	6
AO7(mmol L^{-1})	1.00	–	2.00	–	1.00	2.00
AG25(mmol L^{-1})	–	1.00	–	2.00	1.00	2.00

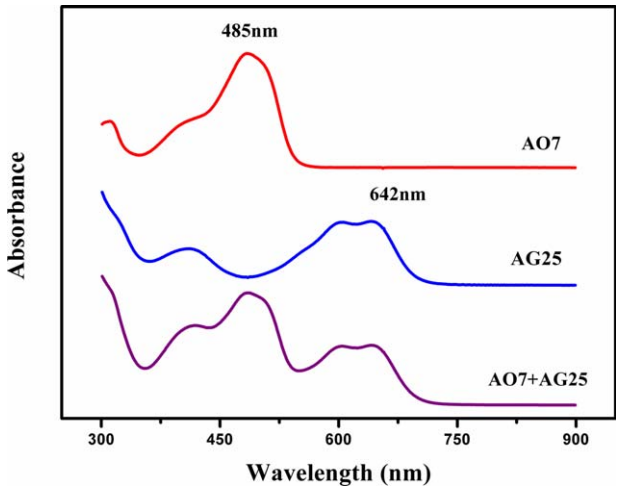

Figure 2. The UV/visible spectra of AO7, AG25 and mixture solution (AO7+AG25). [Color figure can be viewed in the online issue, which is available at wileyonlinelibrary.com.]

$$q_e = \left(\frac{(C_0 - C_e) \times V}{m}\right) \quad (1)$$

where q_e is the sorption capacity of absorbent (mmol g^{-1}), C_0 and C_e are the initial and equilibrium solution concentration (mmol L^{-1}), V is the volume of solution (L), and m is the dose of absorbent (dry basis, g).

Assuming there is no interaction between AO7 and AG25, the total absorbance of a binary component solution can be expressed by eq. (2). The concentration of each dye in a mixture of the two dyes can be calculated using eq. (3) and eq. (4). The adsorption capacity of each dye can then be determined.

$$A_{\lambda mix} = A_{\lambda AO7} + A_{\lambda AG25} \quad (2)$$

$$A_{485(mix)} = \varepsilon_{485(AO7)} C_{AO7} + \varepsilon_{485(AG25)} C_{AG25} \quad (3)$$

$$A_{642(mix)} = \varepsilon_{642(AO7)} C_{AO7} + \varepsilon_{642(AG25)} C_{AG25} \quad (4)$$

where $A_{\lambda mix}$, $A_{\lambda AO7}$, and $A_{\lambda AG25}$ are the absorbance of mixture solution, AO7 and AG25 at wavelength λ, respectively. $\varepsilon_{485(AO7)}$, $\varepsilon_{485(AG25)}$, $\varepsilon_{642(AO7)}$, and $\varepsilon_{642\ (AG25)}$ are the calibration constants for pure AO7 and AG25 at wavelength 485 nm and 642 nm, respectively. C_{AO7} and C_{AG25} are the concentration of AO7 and AG25 in mixture solution (mmol L^{-1}). The UV/visible spectra of AO7, AG25, and mixture solution (AO7 and AG25) are shown in Figure 2.

Adsorption isotherms give a good indication of how adsorbates interact with adsorbents. In a binary component system of dye solution, the interaction of two dye molecules may mutually influence the adsorption capacity of adsorbents. Thus, the adsorption equilibrium test was applied to investigate the effect of multisolute interaction on the sorption capacity of CTSN-beads. Sorption of AO7 and AG25 from dye solutions (varied from 0.25 mmol L^{-1} to 3 mmol L^{-1}) was studied in batch experiments at a pH value of 4.0 for 24 h.

Two adsorption isotherms were employed to fit the experimental data:

Langmuir isotherm equation,[27]

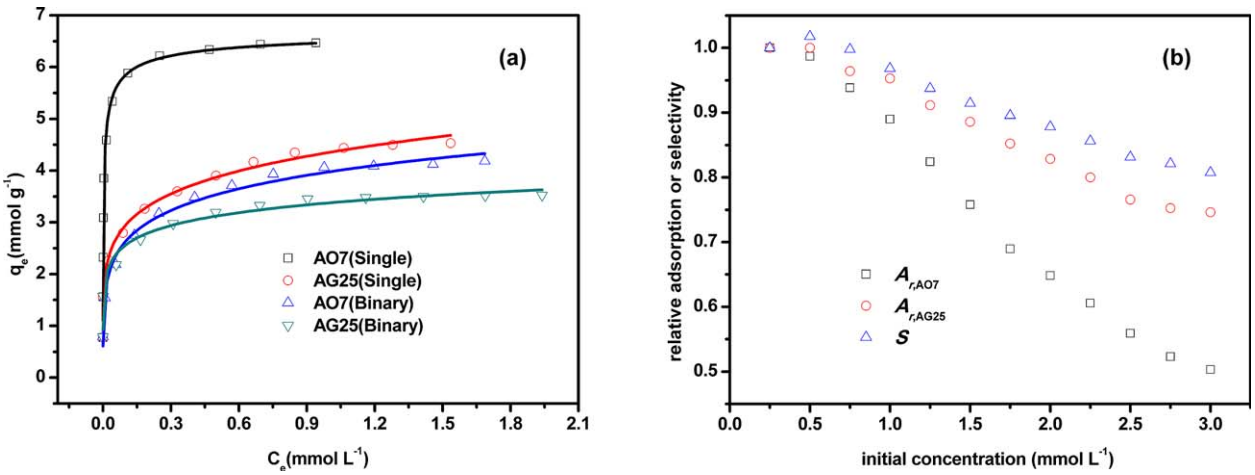

Figure 3. (a) Adsorption isotherms fitted to Freundlich equation (the real lines) (b) Adsorption selectivity in binary system and the variation of relative adsorption of AO7 and AG25. [Color figure can be viewed in the online issue, which is available at wileyonlinelibrary.com.]

$$q_e = \frac{abC_e}{1+bC_e} \tag{5}$$

Freundlich isotherm equation,[28]

$$q_e = K_F C_e^{1/n} \tag{6}$$

where a (mmol g^{-1}) and b (L mmol^{-1}) are the Langmuir isotherm parameters; K_F (mmol$^{1-1/n}$ L$^{1/n}$ g^{-1}) and $1/n$ are Freundlich constants that indicate the extent of sorption and the sorption effectiveness. Models are applied to adsorption data of each dye from single and binary component systems, neglecting the possible interaction from other solutes.

To further study the interaction between AO7 and AG25, formulas (7) and (8) were introduced to compute the relative adsorption capacity[29] of AO7 and AG25 onto CTSN-beads in binary component system.

$$A_r = \frac{[q_C]_B}{[q_C]_S} \tag{7}$$

where $[q_C]_B$ and $[q_C]_S$ are the adsorption capacity of specific adsorbate in the binary component system and in the single component system at the same initial concentration C, respectively. As for binary adsorption system, the selectivity adsorption of dyes on CTSN-beads is calculated using the following equation:

$$S = \frac{[q_{C,AG25}]_B}{[q_{C,AO7}]_B} \tag{8}$$

where $[q_{C,AG25}]_B$ and $[q_{C,AO7}]_B$ are adsorption capacity of AG25 and AO7 in the binary component system at same initial concentration C, respectively.

The pH value of the mixture solution is one of the important factors that affect the interaction between CTSN-beads and dyes. The H+ of the solution influences not only the surface charge of CTSN-beads but also the structural stability of dyes. Electrostatic attraction during the adsorption process is significantly affected by the acidity of the solution. Thus, the influences of pH (varied from 3 to 12) on the sorption were observed. The mixture of CTSN-beads (0.016 dry basis of adsorbents) and dye solution were shaken in flasks for 24 h.

The contact time between adsorbate and adsorbent is of fundamental importance for evaluating an adsorption system. The competition of AO7 and AG25 in the adsorption procedure is also worth investigation. To study the sorption kinetics, CTSN-beads (0.064 g dry basis), and dye solutions (200 mL) were mixed in a shaking isothermal bath for 48 h. Pseudo-first-order[30] and pseudo-second-order[31] equations were applied to analyze the experimental data as follows:

$$\text{Pseudo-first-order}: q_t = q_e(1-e^{-k_1 t}) \tag{9}$$

Table II. Parameters of Langmuir and Freundlich Isotherms for Acid Dyes Adsorption onto CTSN-Beads

	Langmuir isotherm			Freundlich isotherm		
Dye	a(mmol g^{-1})	b(L mmol^{-1})	R^2	K_F(mmol$^{1-1/n}$ L$^{1/n}$ g^{-1})	n	R^2
AO7 (Single)	6.0181	339.01	0.8998	7.1784	4.9554	0.9945
AG25 (Single)	4.3691	28.75	0.7816	4.3531	5.9137	0.9917
AO7 (Binary)	4.1015	22.05	0.8717	3.9784	5.4318	0.9857
AG25 (Binary)	3.5117	27.72	0.6391	3.3784	7.6628	0.9754

Table III. The Sequential Adsorption Experiment Results (C_{rAO7} is the Amount of Desorbed AO7)

	1st time	2nd time	
Initial dye concentration	q_{eAO7} (mmol g^{-1})	q_{eAG25} (mmol g^{-1})	C_{rAO7} (mmol g^{-1})
AO7(1 mmol L^{-1})	3.07	2.74	0.30
AO7(2 mmol L^{-1})	5.65	4.60	1.02

$$\text{Pseudo}-\text{second}-\text{order}: q_t = \frac{k_2 q_e^2 t}{1+k_2 q_e t} \quad (10)$$

where k_1 (min^{-1}) and k_2 (g $mmol^{-1}$ min^{-1}) are the rate constants for the pseudo-first-order and pseudo-second-order equations, respectively. q_t (mmol g^{-1}) and q_e (mmol g^{-1}) are the amount of dye absorbed at time t(min) and at equilibrium. The initial adsorption rate h (mmol g^{-1} min^{-1}) can be calculated as follows:

$$h = k_2 q_e^2 \quad (11)$$

and the intraparticle diffusion equation for biosorption system was also introduced as follows[32]:

$$q_t = k_d t^{1/2} + I \quad (12)$$

where k_d is the intraparticle diffusion constant (mmol g^{-1} $min^{-1/2}$), I is the intercept (mmol g^{-1}).

Temperature is an important factor affecting chitosan adsorption. Temperature influences not only the capacity of adsorbents but also the mass transfer process of adsorbates. Thus, the adsorption behaviors of AO7 and AG25 onto CTSN-beads at different temperatures (varied from 298K to 338K) were also investigated.

RESULTS AND DISCUSSION

Adsorption Equilibrium

Figure 3(a) shows the adsorption isotherms of single and binary dyes using CTSN-beads. The parameters of adsorption models obtained by nonlinear regression analysis are listed in Table II. The Freundlich isotherm was found to provide a better theoretical correlation of the experimental data for sorption, which suggests that the adsorption of acid dyes onto CTSN-beads is multilayer adsorption and the adsorption surface is heterogeneous.[33] It is worth noting that the Freundlich isotherm can also provide an acceptable fits for dyes from binary component system. All values of n are more than 1, which shows that adsorption conditions are favorable.[34] Comparing the K_F of dyes from a single component system, the sorption capacity of CTSN-beads for AO7 is much greater than that for AG25, which could be attributed to the larger molecular size of AG25 than that of AO7. The large size of AG25 makes it difficult to diffuse into the CTSN-bead matrix. Furthermore, more sulfate groups in the AG25 molecule might occupy more protonated amine groups, which would reduce the adsorption capacity. Similar results were reported for the adsorption of metanil yellow and RB15 by Chiou and Chuang.[35] As indicated in Table II, the adsorption capacity of both AO7 and AG25 was reduced in a binary component system, suggesting the existence of competitive adsorption. The adsorption capacity of AO7 and AG25 in a binary component system decreased by 45% and 22%, respectively, compared with the experimental value in a single dye system. The difference in reduction could be attributed to the steric hindrance between the two dyes molecules. The AG25 molecules absorbed onto the CTSN-beads, due to the large molecule size, block more adsorption sites that could be accessible to bind AO7 molecule, thereby greatly affecting the sorption capacity of CTSN-beads for AO7. On the contrary, the smaller AO7 molecule has a limited influence on the AG25 molecule.

Table IV. The Sequential Adsorption Experiment Results (C_{rAG25} Is the Amount of Desorbed AG25)

	1st time	2nd time	
Initial dye concentration	q_{eAG25} (mmol g^{-1})	q_{eAO7} (mmol g^{-1})	C_{rAG25} (mmol g^{-1})
AG25(1 mmol L^{-1})	2.92	1.99	0.03
AG25(2 mmol L^{-1})	5.22	1.54	0.12

Figure 3(b) depicted the adsorption selectivity in a binary component system and the relative adsorption capacity variation of AO7 and AG25 with initial concentration. It was found that both $A_{r,AO7}$ and $A_{r,AG25}$ decreased with increasing initial concentration, and the $A_{r,AO7}$ decreased more drastically than $A_{r,AG25}$, which suggests that a high initial concentration of AG25 resulted in significant competition and AG25 greatly hindered the adsorption of AO7 onto the CTSN-beads. Thus the adsorption capacity of AO7 in binary component system is much lower than that in a single component system. This result is in agreement with the previous conclusion above. In addition, the adsorption selectivity in a binary component system decreased slowly as initial concentration increased, which indicates that AO7 could be more accessible to diffuse into the internal structure of CSTN-beads at high initial concentrations.

Contrast experiments were performed to further verify the existence of steric hindrance in the adsorption process. The contrasting experiments consisted of two sections, namely A and B. In Experiment A, a fixed amount of CTSN-beads were firstly loaded by AO7 (1 mmol L^{-1} and 2 mmol L^{-1}), followed by adsorbing AG25 at the same concentration. Likewise, in Experiment B, CTSN-beads reacted with AG25 (1 mmol L^{-1} and 2 mmol L^{-1}) and AO7 in sequence. As was shown in Tables III and IV, the adsorption capacity of both AG25 and AO7 in Experiment A is much higher than in Experiment B, particularly at high initial concentrations. This result strongly supports the previous conclusion that the adsorbed AG25 can weaken the adsorption of AO7 effectively. Moreover, the value of C_{rAG25} is lower than C_{rAO7}, suggesting that AG 25 displays better adsorption stability than AO7.

Effect of pH

Figure 4 shows the effect of pH on the adsorption of acid dyes onto CTSN-beads and the sorption capacity of CTSN-beads diminishes slowly when pH is increased from 3 to 10, whereas a sharp decrease was observed over the pH range from 10 to 12.

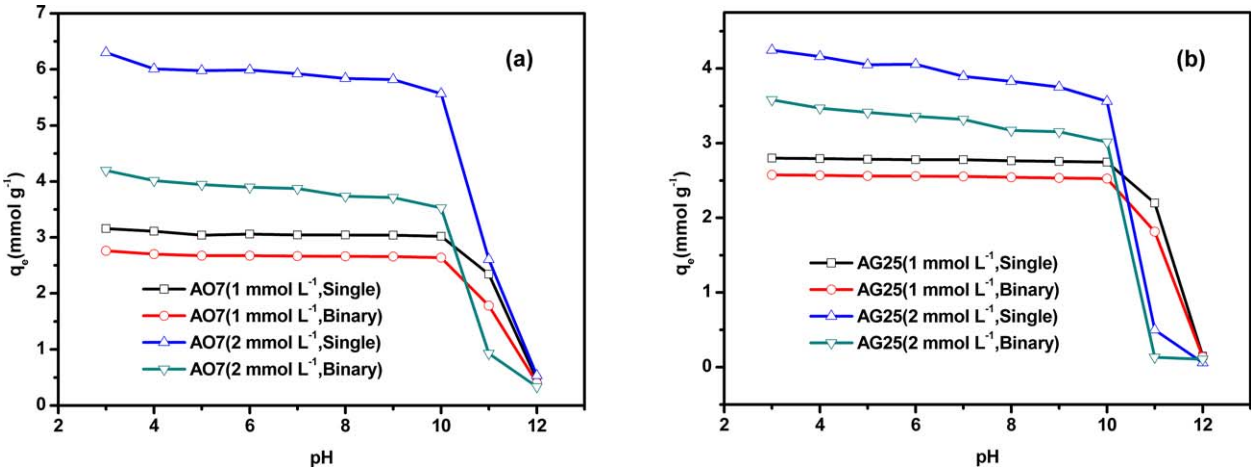

Figure 4. Effect of pH on acid dyes adsorption on to CTSN-beads (a) AO7 (b) AG25. [Color figure can be viewed in the online issue, which is available at wileyonlinelibrary.com.]

This result implies that the adsorption process of dyes onto CTSN-beads is based upon electrostatic attraction. A similar pH-dependent trend was also reported by Wong and Szeto.[36] The progress of adsorption is shown from formula (13) to (15). In an acidic medium, the amino groups ($-NH_3^+$) of CTSN-beads are protonated, which is favorable for attracting the sulfonic acid groups (SO_3^-) of dyes. Under basic conditions, the sorption ability decreases sharply because of the deprotonation of active groups. Comparing the results at different initial concentrations, the sorption capacity (q_e) at low initial concentrations remains relatively stable for solutions within a pH range of 3–10 as a result of the sufficient reactive groups. As for each dye, the variation curve of adsorption capacity with pH in the single component system is similar to that in the binary component system, which suggests that pH has no significant impact on the interaction between AO7 and AG25. Both AO7 and AG25 are acid dyes with same sulfonic acid groups; thereby, the effects of pH on the two dyes are equal. The desorption of CTSN-beads also has been investigated. 1 mmol L^{-1} Na_2SO_4/NaOH (pH 12.0) solution was chosen to regenerate the CTSN-beads. The desorption agent can efficiently remove absorbed dyes (90.2% AO7 and 84.4% AG25 for single system, 89.1% AO7 and 80.9% AG25 for single system). The results indicated that the CTSN-beads can be recovered for consecutive uses.

$$\text{R-NH}_2 + \text{H}^+ \underset{}{\overset{\text{Protonation}}{\rightleftharpoons}} \text{R-NH}_3^+ \quad (13)$$

$$\text{dye-SO}_3\text{Na} \xrightarrow[\text{Dissociation}]{\text{H}_2\text{O}} \text{dye-SO}_3^- + \text{Na}^+ \quad (14)$$

$$\text{R-NH}_3^+ + \text{dye-SO}_3^- \overset{\text{Electrostatic interaction}}{\rightleftharpoons} \text{R-NH}_3^+ \ldots {}^-\text{O}_3\text{S-dye} \quad (15)$$

Sorption Kinetics

Figure 5 illustrates the sorption kinetics of AO7 and AG25 in single and binary component system. Rapid uptake was observed during the initial stage and equilibrium was reached within 48 h. The dynamic model parameters and correlation coefficients obtained by nonlinear fitting are listed in Table V. Higher correlation coefficients (above 0.9667 for single system, above 0.9694 for binary system) were obtained from the pseudo-first-order adsorption model than that from the pseudo-second-order adsorption model, which indicates that the pseudo-second-order adsorption mechanism is predominant

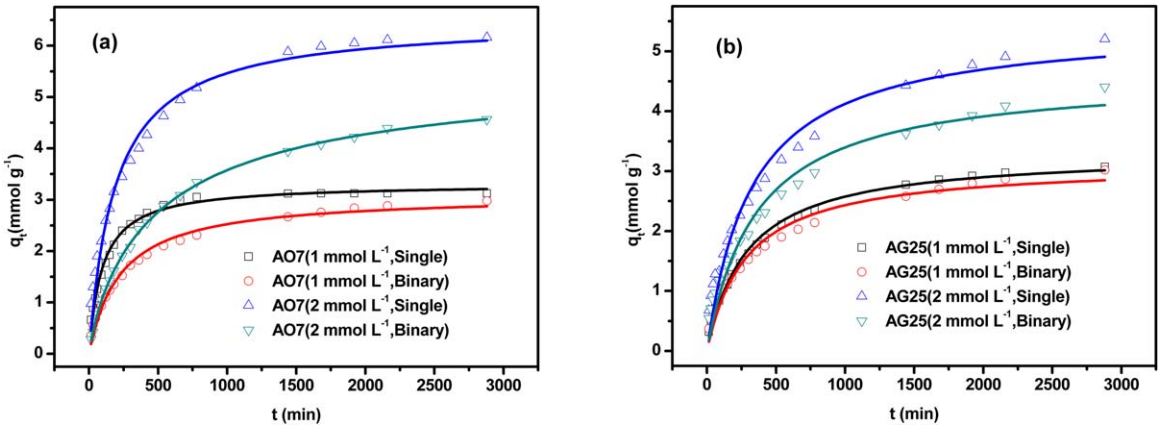

Figure 5. Effect of contact time on acid dyes adsorption (the real lines represent modeled results using the pseudo-second-order equation). (a) AO7 (b) AG25. [Color figure can be viewed in the online issue, which is available at wileyonlinelibrary.com.]

Table V. Parameters of Kinetic Models for AO7 and AG25 Adsorption onto CTSN-Beads

	Pseudo-first-order			Pseudo-second-order			
Dye	$k_1 \times 10^3$ (min^{-1})	q_e (mmol g^{-1})	R^2	$k_2 \times 10^3$ (g $mmol^{-1}$ min^{-1})	q_e (mmol g^{-1})	H (mmol g^{-1} min^{-1})	R^2
AO7(1 mmol L^{-1}, Single)	7.40	3.0234	0.9633	3.19	3.3125	0.0350	0.9908
AO7(1 mmol L^{-1}, Binary)	3.51	2.7204	0.9454	1.42	3.0965	0.0137	0.9853
AO7(2 mmol L^{-1}, Single)	4.02	5.7794	0.9362	1.02	6.4957	0.0430	0.9820
AO7(2 mmol L^{-1}, Binary)	2.32	4.2545	0.9827	0.86	5.6452	0.0273	0.9994
AG25(1 mmol L^{-1}, Single)	2.91	2.8639	0.9639	1.05	3.3153	0.0115	0.9897
AG25(1 mmol L^{-1}, Binary)	2.86	2.7136	0.9311	1.11	3.1298	0.0109	0.9735
AG25(2 mmol L^{-1}, Single)	2.59	4.6924	0.9277	0.57	5.4582	0.0169	0.9667
AG25(2 mmol L^{-1}, Binary)	2.42	3.9250	0.9343	0.61	4.6121	0.0129	0.9694

in both single and binary component systems, and chemisorption controls the dye adsorption process.[37] The $q_{e,cal}$ value is consistent with experimental data. The larger value of initial sorption h for AO7 than for AG25 demonstrates that AO7, with the smaller molecular size, not only increases the concentration of dye on the surface of CTSN-beads but also promotes mass transfer. The chemical structure of AO7 presents a more compatible size and stereo structure with CTSN-beads compared with AG25. Similar results were found by Wang.[38] Furthermore, the h for AO7 in a binary component solution is much lower than for a single component solution, especially at a higher initial concentration (2 mmol L^{-1}). Whereas, the h for AG25 in a binary component solution is slightly lower than that in a single component solution. This difference indicates that the AG25 adsorbed onto CTSN-beads weaken both the adsorption capacity and the mass transfer of AO7. The relative adsorption and selectivity of CTSN-beads for the two dyes were depicted in Figure 6. Evidently, the adsorption process could be divided into two stages. In the first 500 min, the curve decreased sharply, which may explain why AG25 exhibited a strong disincentive for the adsorption of AO7, which is also in agreement with the previous discussion above. With the lapse of time, the sorption rate of AO7 increased slightly, which could be attributed to its smaller molecular size, which endows it with excellent diffusion performance. Conversely, the adsorption of AG25 in binary component system was slightly affected by AO7.

Intraparticle diffusion may also be involved in the adsorption processes. Fitting by the intraparticle diffusion equation are shown in Figure 7, and the constants are listed in Table VI. According to Mahmoodi,[23] if the plot passes through the origin, the intraparticle diffusion would be the only rate-controlling step. Otherwise, there are likely other mechanisms involved in the adsorption process. Figure 7 shows the three steps, each controlled by different mechanisms. (1) The first sharp stage indicates the mass transfer of solute molecules, including boundary layer diffusion and the diffusion from bulk solution to the outer surface of adsorbent. As listed, all diffusion constants, k_{d1}, for AO7 are higher than those for AG25 under the same condition (Table VI), suggesting that AO7, with its smaller molecular size, increases the concentration of dye on the surface

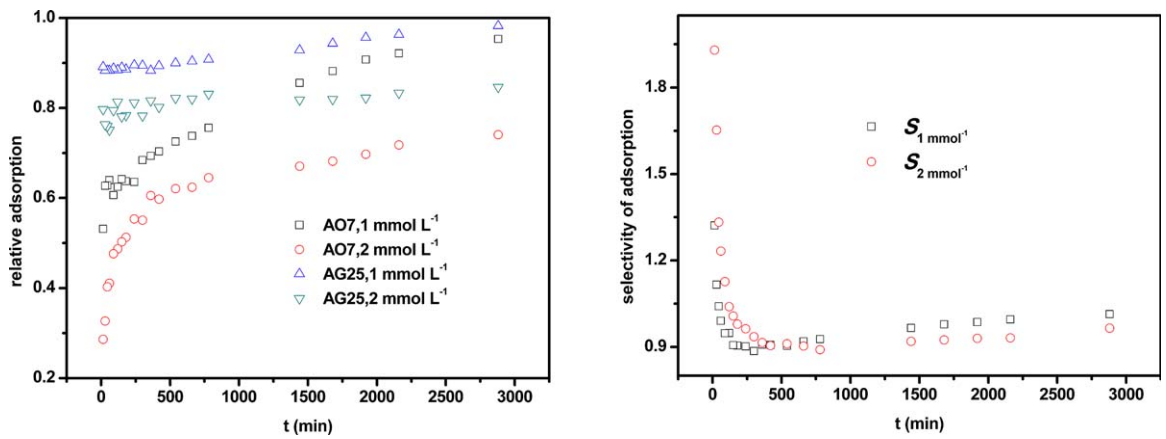

Figure 6. The relative adsorption and selectivity of sorption kinetics. [Color figure can be viewed in the online issue, which is available at wileyonlinelibrary.com.]

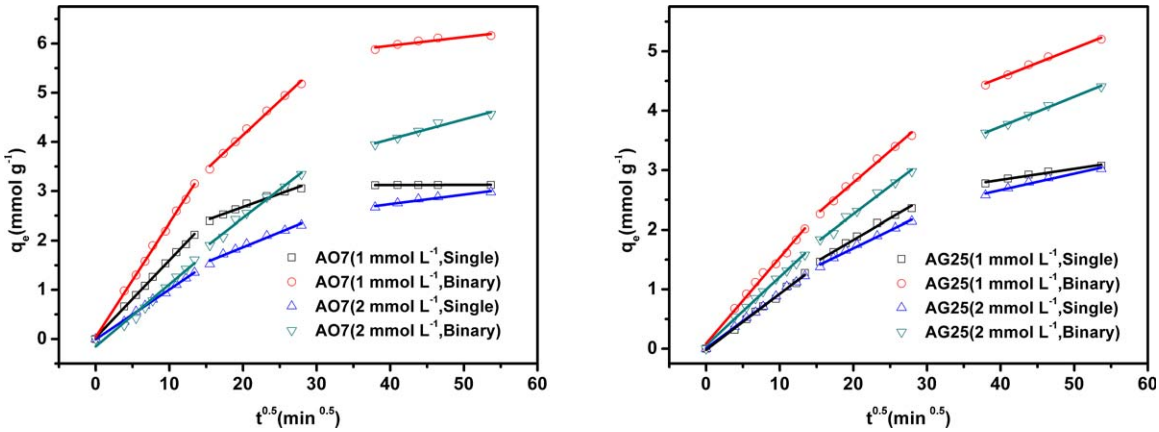

Figure 7. The plot of intraparticle diffusion modeling of AO7 and AG25. [Color figure can be viewed in the online issue, which is available at wileyonlinelibrary.com.]

of adsorbent beads, which exhibits a stronger driving force for this adsorption period. Furthermore, all k_{d1} for AO7 in mixture solution are much smaller than those in a single component system. This result also supports the assertion that steric effects slow down the adsorption rate of AO7 dramatically. (2) The second portion described the gradual adsorption process, which could be attributed to intraparticle diffusion. At the higher initial concentration (2 mmol L^{-1}), the k_{d2} for AO7 is higher than for AG25, which indicates the diffusion advantage of AO7 over AG25. However, at the lower initial concentration (1 mmol L^{-1}) of dye, the values of kd2 for AO7 are less than those for AG25. Most AO7 molecules were adsorbed onto the surface of the adsorbent and the adsorption sites were occupied at the first adsorption stage, therefore, only a small amount of AO7 molecules were loaded at the second stage due to the lack of sorption sites, which likely led to a slower transfer rate. (3) The last portion depicts the final equilibrium stage, where the residual concentration of dyes became extremely low. The minimal amounts of dyes and the exhausted adsorption sites greatly weaken the external mass transfer and intraparticle diffusion, as well as the reaction rate. Similar results were reported in other literature sources.[39,40]

Effect of Adsorption Temperature

Figure 8 shows the effect of temperature on the adsorption of acid dyes onto the CTSN-beads. It could be observed from Figure 8(a) that the adsorption capacities of CTSN-beads in a single component system is enhanced as the increasing temperature, which might be attributed to the dimensions of the pores on CTSN-beads became large at higher temperatures,[41] and the larger pore sizes can provide more adsorption sites for dyes. Another explanation is that the boundary layer effect is weakened owing to the higher temperatures.[42] As depicted in Figure 8(b), it is interesting to note that the trends of adsorption capacities in a binary component system are different from that in a single component system. With increasing temperatures, the adsorbed amount of dye at the lower initial concentration (1 mmol L^{-1}) increases, whereas, it reduces AO7 in a binary component system at the higher initial concentration (2 mmol L^{-1}). This difference may be ascribed to the insufficient adsorption sites caused by competitive adsorption. The higher temperatures greatly accelerate the diffusion and sorption rates for AG25, which impedes the reaction between CTSN-beads and AO7. On the other hand, AG25 is accessible for generating more stable bonds with the active sites on CTSN-beads when compared with AO7, as a result of the two sulfonate groups in the AG25 molecule. Thus, the adsorbed

Table VI. Parameters of Intraparticle Diffusion Model for AO7 and AG25 Adsorption onto CTSN-Beads

Dye	k_{d1}(mmol g^{-1} min$^{-1/2}$)	R^2	k_{d2}(mmol g^{-1} min$^{-1/2}$)	R^2	k_{d3}(mmol g^{-1} min$^{-1/2}$)	R^2
AO7(1 mmol L^{-1}, Single)	0.1571	0.9990	0.0538	0.9745	0.0003	0.9643
AO7(1 mmol L^{-1}, Binary)	0.1014	0.9980	0.0610	0.9750	0.0193	0.9476
AO7(2 mmol L^{-1}, Single)	0.2314	0.9982	0.1395	0.9934	0.0174	0.9454
AO7(2 mmol L^{-1}, Binary)	0.1263	0.9751	0.1155	0.9864	0.0404	0.9547
AG25(1 mmol L^{-1}, Single)	0.0944	0.9955	0.0724	0.9872	0.0187	0.9635
AG25(1 mmol L^{-1}, Binary)	0.0917	0.9982	0.0603	0.9879	0.0277	0.9635
AG25(2 mmol L^{-1}, Single)	0.1446	0.9911	0.1066	0.9906	0.0491	0.9887
AG25(2 mmol L^{-1}, Binary)	0.1151	0.9955	0.0942	0.9874	0.0503	0.9952

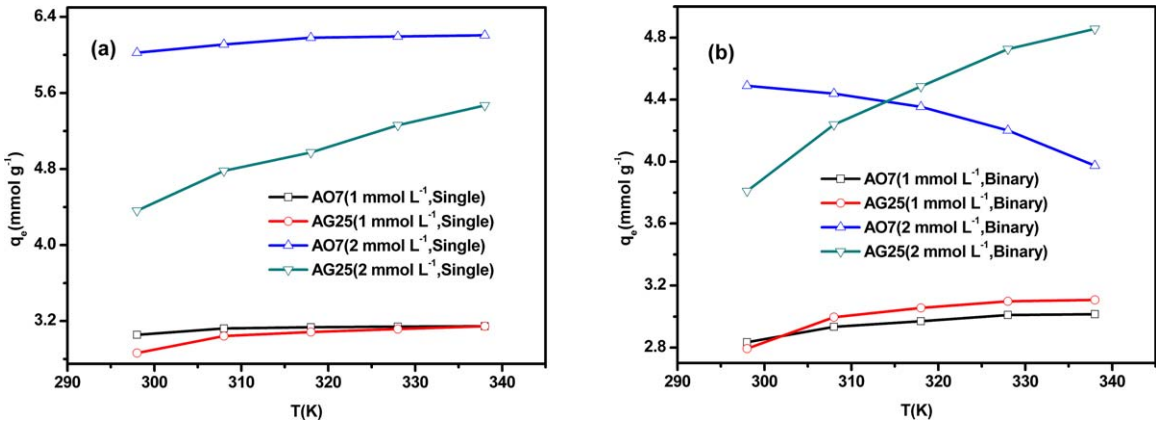

Figure 8. Effect of temperature on acid dyes adsorption by CTSN-beads (a) Single system (b) Binary system. [Color figure can be viewed in the online issue, which is available at wileyonlinelibrary.com.]

AO7 onto CTSN-beads tend to be replaced by AG25, particularly at high temperatures. Al-Degs[43] also discovered similar replacement between reactive yellow and reactive black B.

CONCLUSIONS

In this study, the CTSN-beads were applied to investigate the interaction between AO7 and AG25 during adsorption processes. The Freundlich isotherm was found to provide a better theoretical correlation of the experiment data for both single and binary component systems. The relative and selectivity analyses proved the existence of steric hindrance between AO7 and AG25. The adsorption period of acid dyes onto CTSN-beads is pH-dependent and based upon electrostatic attraction. The pseudo-second-order model agrees very well with kinetic experiment data, indicating that the chemisorption is rate-controlling step during sorption procedure. Relevant experiments also demonstrate that the adsorption capacities and rate are directly related to the molecular size of the dyes. The adsorbed AG25 weaken the adsorption capacity of AO7 onto CTSN-beads, as well as the mass transfer of AO7. Additionally, the intraparticle diffusion model demonstrated that there are three steps in the adsorption processes, which were controlled by different diffusion mechanisms. High temperature is generally favorable to the adsorption capacity of CTSN-beads in single component systems. Nevertheless, the uptake capacity of AO7 in a binary component system declined at higher temperatures as a result of insufficient adsorption sites caused by competitive adsorption.

ACKNOWLEDGMENTS

This work was supported by Experimental Chemistry Center Tongji University, Shanghai. The authors thank XiaoWei Yi for assistance during this work and Prof. Dongbei Wu for language help.

REFERENCES

1. Crini, G. *Bioresour. Technol.* **2006**. *97*, 1061.
2. Yahagi, T.; Degawa, M.; Seino, Y.; Matsushima, T.; Nagao, M.; Sugimura, T.; Hashimoto, Y. *Cancer Lett.* **1975**, *1*, 91.
3. Chowdhury, S.; Mishra, R.; Saha, P.; Kushwaha, P. *Desalination* **2011**, *265*, 159.
4. Gupta, V. K.; Gupta, B.; Rastogi, A.; Agarwal, S.; Nayak, A. *J. Hazard. Mater.* **2011**, *186*, 891.
5. Sun, H. M.; Cao, L. Y.; Lu, L. H. *Nano Res.* **2011**. *4*, 550.
6. Gupta, V. K.; Jain, R.; Mittal, A.; Saleh, T. A.; Nayak, A.; Agarwal, S.; Sikarwar, S. *Mater. Sci. Eng. C-Bio. S* **2012**, *32*, 12.
7. Cheng, S. Y.; Oatley, D. L.; Williams, P. M.; Wright, C. J. *Water Res.* **2012**. *46*, 33.
8. Pelaez, M.; Nolan, N. T.; Pillai, S. C.; Seery, M. K.; Falaras, P.; Kontos, A. G.; Dunlop, P. S. M.; Hamilton, J. W. J.; Byrne, J. A.; O'Shea, K.; Entezari, M. H.; Dionysiou, D. D. *Appl. Catal. B-Environ* **2012**, *125*, 331.
9. Verma, A. K.; Dash, R. R.; Bhunia, P. *J. Environ. Manage.* **2012**, *93*, 154.
10. Volesky, B. *Water Res.* **2007**, *41*, 4017.
11. Crini, G.; Badot, P.-M. *Prog. Polym. Sci.* **2008**, *33*, 399.
12. Poon, L.; Wilson, L. D.; Headley, J. V. *Carbohydr. Polym.* **2014**, *109*, 92.
13. Reddy, D. H.; Lee, S. M. *Adv. Colloid Interfac.* **2013**, *201-202*, 68.
14. Kyzas, G. Z.; Lazaridis, N. K.; Kostoglou, M. *Chem. Eng. J.* **2014**, *248*, 327.
15. Horinaka, J.-i.; Urabayashi, Y.; Takigawa, T.; Ohmae, M. *J. Appl. Polym. Sci.* **2013**, *130*, 2439.
16. Khalil, M. M. H.; Al-Wakeel, K. Z.; Rehim, S. S. A. E.; Monem, H. A. E. *J. Environ. Chem. Eng.* **2013**, *1*, 566.
17. Yan, Y.; Xiang, B.; Li, Y.; Jia, Q. *J. Appl. Polym. Sci.* **2013**, *4090*.
18. Noroozi, B.; Sorial, G. A.; Bahrami, H.; Arami, M. *Dyes. Pigments* **2008**, *76*, 784.
19. Allen, S. J.; McKay, G.; Porter, J. F. *J. Colloid Interf. Sci.* **2004**, *280*, 322.
20. Fernandez, M. E.; Nunell, G. V.; Bonelli, P. R.; Cukierman, A. L. *Bioresour. Technol.* **2012**, *106*, 55.
21. Wang, S.; Ariyanto, E. *J. Colloid Interf. Sci.* **2007**, *314*, 25.

22. Choy, K. K.; Porter, J. F.; McKay, G. *Langmuir* **2004**, *20*, 9646.
23. Mahmoodi, N. M.; Salehi, R.; Arami, M. *Desalination* **2011**, *272*, 187.
24. Reddy, D. H. K.; Lee, S. M. *J. Appl. Polym. Sci.* **2013**, *130*, 4542.
25. Gonçalves, J. O.; Duarte, D. A.; Dotto, G. L.; Pinto, L. A. A. *CLEAN - Soil, Air, Water* **2013**, *42*, 767.
26. Noroozi, B.; Sorial, G. A. *J. Environ. Sci.* **2013**, *25*, 419.
27. Ho, Y.; McKay, G. *Chem. Eng. J.* **1998**, *70*, 115.
28. Reddad, Z.; Gerente, C.; Andres, Y.; LeCloirec, P. *Environ. Sci. Technol.* **2002**, *36*, 2067.
29. Zou, W.; Bai, H.; Gao, S. *J. Chem. Eng. Data*. **2012**, *57*, 2792.
30. Dinkova-Kostova, A. T.; Holtzclaw, W. D.; Cole, R. N.; Itoh, K.; Wakabayashi, N.; Katoh, Y.; Yamamoto, M.; Talalay, P. *Proc. Natl. Acad. Sci. USA* **2002**, *99*, 11908.
31. Ho, Y. S.; McKay, G. *Process. Biochem.* **1999**, *34*, 451.
32. Ho, Y. S.; Ng, J. C. Y.; McKay, G. *Sep. Purif. Rev.* **2000**, *29*, 189.
33. Wang, S.; Ng, C. W.; Wang, W.; Li, Q.; Hao, Z. *Chem. Eng. J.* **2012**, *197*, 34.
34. Annadurai, G.; Ling, L. Y.; Lee, J. F. *J. Hazard. Mater.* **2008**, *152*, 337.
35. Chiou, M. S.; Chuang, G. S. *Chemosphere* **2006**, *62*, 731.
36. Wong, Y. C.; Szeto, Y. S.; Cheung, W. H.; McKay, G. *Process. Biochem.* **2004**, *39*, 695.
37. Wong, Y. C.; Szeto, Y. S.; Cheung, W. H.; McKay, G. *Langmuir* **2003**, *19*, 7888.
38. Wang, Z.; Xiang, B.; Cheng, R.; Li, Y. *J. Hazard. Mater.* **2010**, *183*, 224.
39. Kang, Q.; Zhou, W.; Li, Q.; Gao, B.; Fan, J.; Shen, D. *Appl. Clay. Sci.* **2009**, *45*, 280.
40. Chen, C. Y.; Chang, J. C.; Chen, A. H. *J. Hazard. Mater.* **2011**, *185*, 430.
41. Cestari, A. R.; Vieira, E. F.; Pinto, A. A.; Lopes, E. C. *J. Colloid Interf. Sci* **2005**, *292*, 363.
42. Crini, G.; Martel, B.; Torri, G. *Int. J. Environ. Pollut.* **2008**, *34*, 451.
43. Al-Degs, Y.; Khraisheh, M. A. M.; Allen, S. J.; Ahmad, M. N.; Walker, G. M. *Chem. Eng. J.* **2007**, *128*, 163.